Torque Management of Engines with Variable Cam Timing

Mrdjan Jankovic, Florian Frischmuth, Anna Stefanopoulou, and Jeffrey A. Cook

Automotive powertrain control systems are subject to diverse and, usually, conflicting requirements. In particular, exhaust emissions must meet increasingly stringent Federal and California standards while fuel economy must meet customer expectations and contribute to Federally mandated Corporate Average Fuel Economy (CAFE) imperatives. Neither vehicle performance nor reliability may be compromised in attaining these goals (emission performance must be guaranteed for 100,000 miles). Of course, all these objectives must be achieved at the lowest possible cost and with the minimum number of sensors and actuators.

The conventional method of reducing feedgas oxides of nitrogen (NOx) emissions is by the application of exhaust gas recirculation (EGR). Formation of NOx during the combustion process is influenced by air-fuel ratio (A/F) and temperature. These variables are typically adjusted by directing exhaust gas from the high pressure exhaust manifold via a pulse-width modulated valve to the low pressure induction system where it serves to reduce the combustion temperature and dilute the air-fuel mixture in the cylinder. A desirable side-effect is that the presence of inert exhaust gas raises the intake manifold pressure reducing the pumping losses and improving fuel economy. Although effective, the dynamics associated with this system (transport delay, valve and intake manifold dynamics) can result in vehicle performance deterioration.

The variable cam timing (VCT) system with which this paper is concerned addresses both drivability and emissions performance by utilizing an electro-hydraulic mechanism to rotate the camshaft relative to the crankshaft in order to retard the cam timing with respect to the intake and exhaust strokes of the engine. Variable cam timing operation is illustrated in Fig. 1. By retarding the exhaust valve closing further into the intake stroke, more exhaust gas is drawn into the cylinder providing internal exhaust gas recirculation. In this manner, the amount of residual gas trapped in the cylinder at the end of the exhaust stroke is controlled by cam timing, suppressing NOx formation and reducing the pumping losses [1], [9], [14]. Furthermore, this residual contains some unburned hydrocarbons; consequently, retaining it in the cylinder through two combustion cycles also reduces hydrocarbon emissions [8].

In addition to the reduction of NOx and HC emissions, variable cam timing permits the engine designer to optimize cam timing over a wide range of engine operating conditions, providing both good idle quality (minimal overlap between the intake and exhaust events) and improved wide-open throttle performance (maximum inducted charge). In this article, we will assume that the camshaft position is continuously variable to

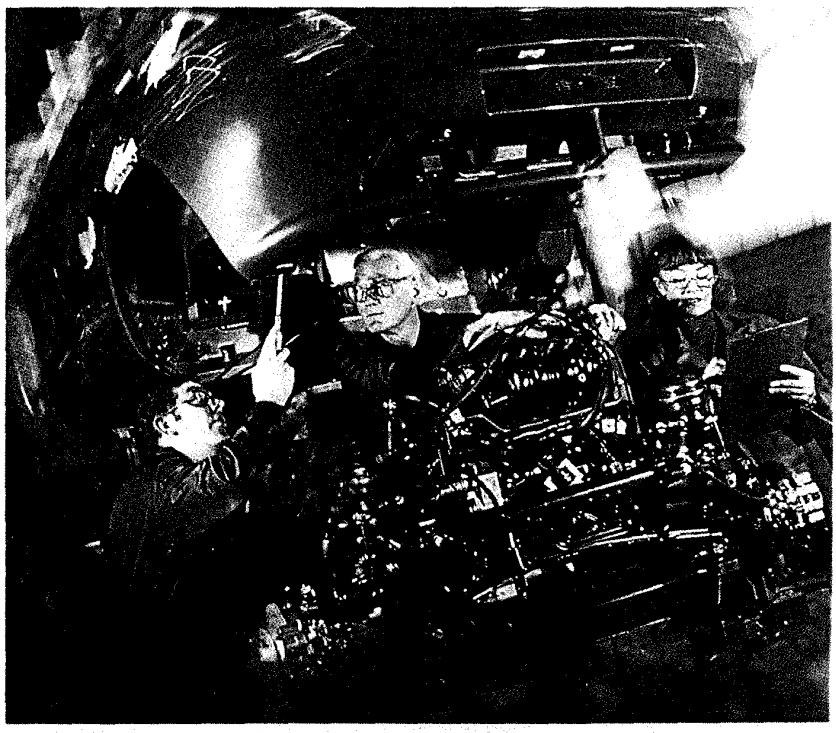

Jankovic, Frischmuth, and Cook are with Ford Research Laboratories, P.O. Box 2053, MD 2036 SRL, Dearborn, MI 48121. Stefanopoulou is with the Dept. of Mechanical and Environmental Engineering, University of California, Santa Barbara, CA 93106.

 0272-1708/98/$10.00©1998IEEE

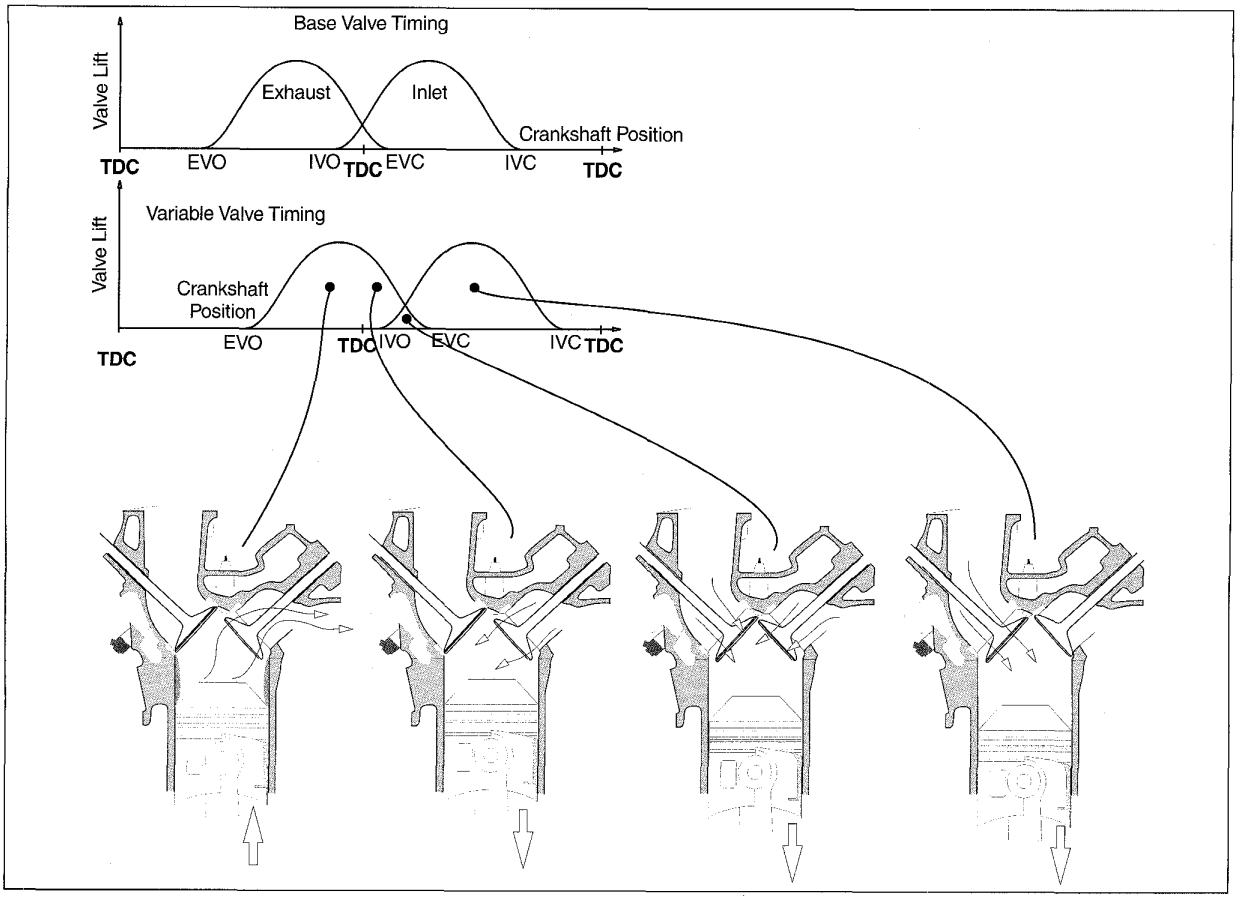

Fig. 1. Valve lift profiles of conventional and VCT engines. By retarding the cam phasing, the exhaust valve stays open during the intake event for a longer time period, retaining otherwise unburned HC and reducing the combustion temperature due to the dilution of the inert gas.

achieve the full benefits in emissions and torque. There are successful examples of simple, two-position VCT systems that address and partially resolve the idle versus wide-open throttle performance trade-off. Obviously, variable cam timing has a substantial effect on the breathing process of the engine. Properly controlled, the variable cam can be used to operate the engine at higher intake manifold pressures, reducing pumping losses at part throttle conditions and providing a fuel economy improvement as well [2], [4], [7].

Four versions of VCT are available for double overhead camshaft (DOHC) engines: phasing only the intake cam (intake only), phasing only the exhaust cam (exhaust only), phasing the intake and exhaust cams equally (dual equal), and phasing the two camshafts independently (dual independent). The dual independent VCT provides the best performance, but it is the most complex and expensive to implement. Of the remaining three, dual equal VCT, where the intake valve timing and exhaust valve timing are advanced or retarded equally, gives the best overall performance in terms of emissions and fuel economy [6]. On the other hand, the dual equal VCT causes the greatest disturbance to cylinder air-charge and air-fuel ratio which may result in drivability problems and increased tailpipe emissions above levels predicted by the steady state analysis [11].

One method of reducing the air-charge variation and improving drivability is to "detune the cam" by slowing down the response of the VCT mechanism. However, detuning the cam results in engine operation with lower levels of recirculated exhaust gas and increased NOx emissions. Drivability can also be improved by selecting a less aggressive (steady-state suboptimal) cam timing schedule, but again the price for this is increased NOx emissions and reduced fuel economy. Instead, in this article we pursue an active method of compensation for cylinder air-charge variation due to VCT which employs either an electronic throttle or an air-bypass valve. Electronic control of the throttle provides an additional degree of control capability to affect emissions and fuel economy while providing the performance desired by the driver as interpreted from the accelerator pedal position. The air-bypass valve is a conventional actuator of limited authority used to admit air flow to the engine under closed throttle operation, and to effect idle speed regulation [3], [5].

From the controller design point of view, several prominent characteristics of this problem will dictate our approach:

- The model of the plant is low order, nonlinear, with known nonlinearities available from the dynamometer mapping data.
- The disturbance (cam phasing) is measured.
- The output (cylinder mass air flow, or cylinder air charge, or torque) is not measured.
- Transient response is much more important than steady state accuracy.

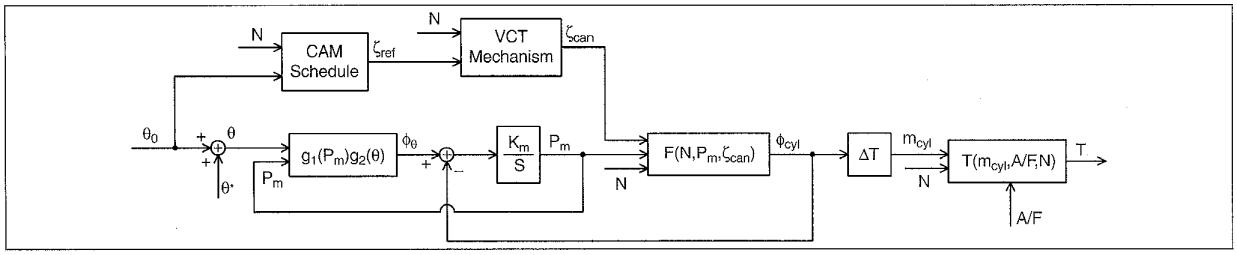

Fig. 2. Engine model with VCT and electronic throttle.

The first three items above suggest that a feedforward compensation may be the most appropriate, so this is the approach we adopt. Our compensator design is based on a low order nonlinear model of a VCT engine derived in [12]. Starting from the nonlinear model we develop a nonlinear control algorithm that rejects the air-charge (torque) disturbance and recovers the drivability of the conventional engine. (Note that the "conventional engine" in this context is the engine which corresponds to fixed cam at 0° (base cam). However, this algorithm requires a degree of control authority which is available only if the engine is equipped with an electronic throttle (ETC). If the engine is equipped only with an air-bypass valve (ABV), the limited control authority of this device forces us to change the design objective: rather than to emulate the conventional engine, our compensation tries to achieve the drivability of an engine with a different characteristic.

Because the relative degree from the disturbance to the output is smaller that the one from the control input to the output (the disturbance is closer to the output than the control), our compensation algorithm uses the derivative of the disturbance (cam phasing). We present two different methods of implementing this term in order to find a trade-off among the performance of the compensator, the sensitivity to measurement noise, and the sensitivity to parameter variation.

VCT Engine Model

The control design engine model described here is a continuous-time nonlinear, low-frequency phenomenological model developed in [10] and modified to incorporate VCT in [12]. Details about the VCT engine model can be found in [13]. A block diagram in Fig. 2 shows the cam timing reference ζ_{ref} scheduled on engine speed and driver demanded throttle θ_0.

Notation

A/F air-fuel ratio
N engine speed
P_m: manifold pressure
m_{cyl}: mass of air into cylinder
T: torque
ζ_{ref}: cam phasing command
ζ_{cam}: cam phasing
θ_0: throttle angle due to driver request
θ^*: additive throttle angle due to compensation
θ: total throttle angle
ϕ_θ: mass air flow rate into manifold
ϕ_{cyl}: mass air flow rate into cylinders
δ: opening of the air-bypass valve
ΔT: duration of the intake event
σ: spark retard from maximum braking torque (MBT) setting.

The engine breathing dynamics describe the filling and emptying of the manifold. The rate of change is proportional to the difference between mass air flow rate into the manifold through the throttle (ϕ_θ) and the mass air flow rate out of the manifold into the cylinders (ϕ_{cyl})

$$\dot{P}_m = K_m(\phi_\theta - \phi_{cyl}). \tag{1}$$

The mass air flow through the throttle body into the manifold is a function of the upstream atmospheric pressure P_a, the manifold pressure, and the throttle angle:

$$\phi_\theta = g_1(P_m / P_a)g_2(\theta, P_a),$$

where

$$g_1(P_m / P_a) = \begin{cases} \gamma^{1/2}\left(\frac{2}{\gamma+1}\right)^{\frac{\gamma+1}{2(\gamma-1)}} & \text{if } \frac{P_m}{P_a} \le \left(\frac{2}{\gamma+1}\right)^{\frac{\gamma}{\gamma-1}} \\ \sqrt{\frac{2\gamma}{\gamma-1}\left(\left(\frac{P_m}{P_a}\right)^{\frac{2}{\gamma}} - \left(\frac{P_m}{P_a}\right)^{\frac{\gamma+1}{\gamma}}\right)} & \text{if } \frac{P_m}{P_a} > \left(\frac{2}{\gamma+1}\right)^{\frac{\gamma}{\gamma-1}} \end{cases}, \tag{2}$$

with $\gamma = c_p/c_v = 1.4$. $g_2(\theta, P_a)$ is the throttle dependent mass air flow characteristic obtained from static engine data. We assume that $P_a = 1$ bar and suppress the dependence of g_1 and g_2 on P_a.

In this application, the throttle angle is comprised of the throttle position due to the driver's request (θ_0) and an additive term due to the compensation (θ^*)

$$\theta = \theta_0 + \theta^*.$$

It is important to observe in Fig. 2 that the cam is scheduled only on θ_0. The mass air flow rate into the cylinders can be represented as a function of cam phasing ζ_{cam}, manifold pressure P_m, and engine speed N:

$$\phi_{cyl} = F(N, P_m, \zeta_{cam}). \tag{3}$$

For our design model we approximate $F(N, P_m, \zeta_{cam})$ by a function linear in P_m:

$$\phi_{cyl} = \alpha_1(N, \zeta_{cam})P_m + \alpha_2(N, \zeta_{cam}), \tag{4}$$

where α_1 and α_2 are low order polynomials in N and ζ_{cam}.

The generation of torque depends on the cylinder air charge m_{cyl}, air-fuel ratio A/F, spark retard from MBT σ, and engine speed. This relationship is best captured by curve fitting of experimental data:

$$T = T(m_{cyl}, A/F, \sigma, N), \tag{5}$$

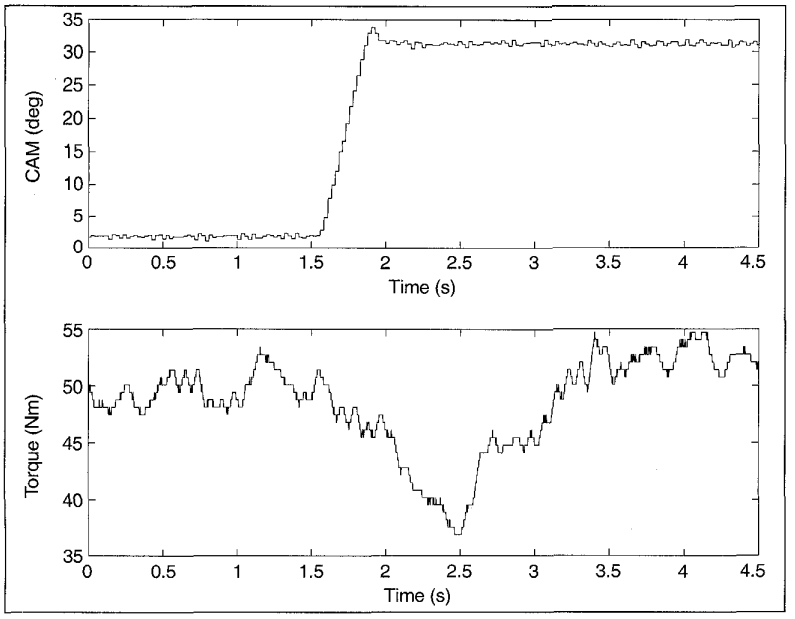

Fig. 3. Engine torque response to a change in cam phasing at fixed throttle and engine speed.

where $m_{cyl} \approx \phi_{cyl}\Delta T$, ($\Delta T$ is the duration of the intake event which depends on engine speed).

In spark ignited (gasoline) engines the air-fuel ratio is maintained at stoichiometry (14.3) in order to ensure that the catalytic converter operates at its peak efficiency. Thus, from the expressions (3) and (5) it is clear that the change in cam timing affects the torque through the change in cylinder mass air flow rate. In sonic flow, when $g_1(P_m) = c$ (c is a constant), the change in ζ_{cam} does not change the steady state value of the torque. This can be verified on the model by noting that, in steady state when $\dot{P}_m = 0$, $\phi_{cyl} = \phi_\theta = cg_2(\theta)$ independently of ζ_{cam}. However, cam transients do affect the torque as one can see in the dynamometer test data in Fig. 3 that show the response of engine torque to a change in ζ_{ref} with the other variables held constant. If the throttle flow is subsonic, cam changes also affect the steady state values of the cylinder mass air flow and torque.

The cam timing has to change depending on the operating conditions. For this reason, ζ_{ref} is scheduled on engine speed and throttle position. Typically, the schedule reaches maximal cam retards at part throttle which provides maximal internal EGR. While close to idle and at wide open throttle the cam phasing is at zero or slightly advanced. Scheduling cam timing on throttle causes it to change when the pedal is depressed or released. The torque variation caused by the cam transient leads to an undesirable engine response and drivability problems. This effect will be illustrated in subsequent sections.

Electronic Throttle Based Compensator

We design a compensator to remove or reduce the effect of the cam transients on the cylinder mass air flow which employs θ^* as a virtual actuator. We assume that the variables available for measurement are the manifold pressure P_m, engine speed N, and the cam position ζ_{cam}. Our design objective is to recover the drivability of the conventional engine.

The basic idea is to find a control law for θ^* such that the rate of change of ϕ_{cyl} coincides with that of the conventional engine. We start with the equations (1) and (3) which describe the manifold filling and engine pumping rates. By differentiating φ_{cyl} we obtain

$$\dot{\phi}_{cyl} = \frac{\partial F(N,P_m,\zeta_{cam})}{\partial N}\dot{N} + \frac{\partial F(N,P_m,\zeta_{cam})}{\partial P_m}\dot{P}_m + \frac{\partial F(N,P_m,\zeta_{cam})}{\partial \zeta_{cam}}\dot{\zeta}_{cam}.$$

To simplify our presentation we shall assume that the $\dot{N}$ term is approximately equal to the corresponding term in the conventional engine; that is, we assume that $\partial F(N,P_m,\zeta_{cam}) / \partial N - \partial F(N,P_{m,0}) / \partial N)\dot{N} \approx 0$. Hence, we suppress the $\dot{N}$-terms in our subsequent derivation. If this assumption does not hold we can redesign our compensator in a straightforward way to account for this additional disturbance term. By using the linear (in P_m) approximation of F and expanding $\dot{P}_m$ we obtain

$$\dot{\phi}_{cyl} = \alpha_1(N,\zeta_{cam})K_m(g_1(P_m)g_2(\theta_0+\theta^*) - \phi_{cyl}) + \left(\frac{\partial \alpha_1}{\partial \zeta_{cam}}P_m + \frac{\partial \alpha_2}{\partial \zeta_{cam}}\right)\dot{\zeta}_{cam}. \quad (6)$$

Now we can use θ^* to cancel the disturbance term proportional to $\dot{\zeta}_{cam}$. This, however, will not achieve complete disturbance rejection because α_1 and P_m depend on ζ_{cam}. To achieve our objective we have to choose θ^* in such a way that ϕ_{cyl} behaves as if it is a cylinder mass flow rate of the conventional engine:

$$\dot{\phi}_{cyl} = \alpha_1(N,0)K_m(g_1(\tilde{P}_m)g_2(\theta_0) - \phi_{cyl})), \quad (7)$$

where $\tilde{P}_m$ is a fictitious reference manifold pressure which should be equal to the manifold pressure of the conventional engine driven with the throttle θ_0 and engine speed N. This reference manifold pressure is generated by

$$\dot{\tilde{P}}_m = K_m(g_1(\tilde{P}_m)g_2(\theta_0) - \alpha_1(N,0)\tilde{P}_m - \alpha_2(N,0)). \quad (8)$$

The expression for θ^* is simplified if we substitute $\alpha_1(N,\zeta_{cam})$ instead of $\alpha_1(N,0)$ in (3). This is justified by the fact that between the maximal and the minimal values of ζ_{cam}, α_1 changes by approximately 20–25% and that α_1 affects mostly the speed of response of ϕ_{cyl}.

To achieve (3) with $\alpha_1(N,\zeta_{cam})$ instead of $\alpha_1(N,0)$, the following equality must be satisfied

$$\alpha_1(N,\zeta_{cam})K_m g_1(P_m)g_2(\theta_0+\theta^*) + \left(\frac{\partial \alpha_1}{\partial \zeta_{cam}}P_m + \frac{\partial \alpha_2}{\partial \zeta_{cam}}\right)\dot{\zeta}_{cam} = \alpha_1(N,\zeta_{cam})K_m g_1(P_m)g_2(\theta_0). \quad (9)$$

Thus, the compensation θ^* should be chosen as

$$\theta^* = g_2^{-1}\left(\frac{\frac{\partial\alpha_1}{\partial\zeta_{cam}}P_m + \frac{\partial\alpha_2}{\partial\zeta_{cam}}}{K_m g_1(P_m)\alpha_1}\dot{\zeta}_{cam} + \frac{g_1(\tilde{P}_m)}{g_1(P_m)}g_2(\theta_0)\right) - \theta_0 . \tag{10}$$

Because the function g_1 changes little in the range of manifold pressures between 0.2 to 0.8 bar, another possible simplification is to use the steady state value $\tilde{P}_m^{ss}(\theta_{0,N})$ instead of the dynamically generated pressure $\tilde{P}_m$. In simulations, a slight degradation in performance is noticeable only at high reference manifold pressures.

Robust stability

The above compensation method uses the information of the engine speed, cam phasing, and manifold pressure to modify the throttle and achieve the drivability of the conventional engine. Even though it is designed as a feedforward compensator, because of its dependence on P_m, there is a feedback component which necessitates stability analysis.

If, for fixed N and θ_0, cam retard causes the steady state manifold pressure to rise into the subsonic region, the compensation will create a different set point at a higher value of manifold pressure. This new set point, denoted by P_m^0, may be sensitive to modeling uncertainties. Below, we propose a simple modification which makes the value of P_m^0 less sensitive to modeling uncertainties and guarantees that it is a stable equilibrium point.

If the functions g_1 and g_2 are known accurately, the implementation of the control law (3) leads to

$$\dot{P}_m = K_m\left(-\frac{\frac{\partial\alpha_1}{\partial\zeta_{cam}}P_m + \frac{\partial\alpha_2}{\partial\zeta_{cam}}}{K_m\alpha_1}\dot{\zeta}_{cam} + g_1(\tilde{P}_m)g_2(\theta_0) - F(N, P_m, \zeta_{cam})\right) \tag{11}$$

In steady state, when $\dot{P}_m$ and $\dot{\zeta}_{cam}$ are zero, $\phi_{cyl} = F(N^{ss}, P_m, \zeta_{cam}^{ss}) = g_1(\tilde{P}_m^{ss})g_2(\theta_0)$, that is, in steady state, the cylinder mass air flow rate of the compensated VCT engine is exactly equal to that of the conventional engine.

To analyze the sensitivity of the compensation method we note that the functions g_1, g_2, α_1 and α_2 can be relatively accurately modeled from the static engine data. The only significant source of sensitivity arises because the function g_1, which is close to 0 at high manifold pressures, appears in the denominator in (10). So we only analyze the effect of modeling errors in g_1 on the steady state pressure P_m^0 and the stability of this equilibrium. To make it distinct from the "true" value g_1, we use $\hat{g}_1$ to denote the subsonic flow correction factor employed in the compensator (10).

The steady state pressure P_m^0 can be obtained by solving

$$0 = \frac{g_1(P_m)}{\hat{g}_1(P_m)}\hat{g}_1(\tilde{P}_m^{ss})g_2(\theta_0) - F(N^{ss}, P_m, \zeta_{cam}^{ss}) . \tag{12}$$

At higher manifold pressures, the solution of (12) is very sensitive to changes in $\hat{g}_1$. We can reduce this sensitivity by intentionally skewing $\hat{g}_1$ so that $\hat{g}_1(P_m) > g_1(P_m)$ when P_m is high, say $P_m \geq 0.75$ bar. This guarantees the existence of a single solution of (12) and forces it to assume a lower value, in the direction of smaller sensitivity of (12). The resulting steady state error in the cylinder mass air flow rate does not affect the drivability.

To analyze the stability of the equilibrium at P_m^0, we define $x = P_m - P_m^0$. With $\dot{\zeta}_{cam} = 0$, the linearization of the manifold pressure dynamics around the equilibrium $P = P_m^0$ results in

$$\dot{x} = \left(\frac{1}{\hat{g}_1^2}\left(\frac{\partial g_1}{\partial P_m}\hat{g}_1 - \frac{\partial\hat{g}_1}{\partial P_m}g_1\right)\hat{g}_1(\tilde{P}_m^{ss})g_2(\theta_0) - \alpha_1\right)x .$$

By our choice of $\hat{g}_1$ we have assured not only that $\hat{g}_1 \geq g_1 \geq 0$, but also that $\left|\partial\hat{g}_1/\partial P_m\right| \leq \left|\partial g_1/\partial P_m\right|$. Since $\partial\hat{g}_1/\partial P_m$ and $\partial g_1/\partial P_m$ are both negative, this implies that $(\partial g_1/\partial P_m)\hat{g}_1 - (\partial\hat{g}_1/\partial P_m)g_1 \leq 0$. Because $\hat{g}_1$, g_2, and α_1 are always positive, the equilibrium $x = 0$ is asymptotically stable. Hence, our compensation creates a single equilibrium P_m^0 which is asymptotically stable.

Simulation results for ETC compensator

To demonstrate the effectiveness of the compensation (10) we have tested it on a model which differs from the one used in the controller design. We have used a simpler design model in order to keep the compensator simple. In addition, this provides some indication of the effects of modeling errors on the performance of the compensator.

To implement $\dot{\zeta}_{cam}$ we have chosen an approximate differentiation

$$\dot{\zeta}_{cam} \approx \frac{s}{\tau s + 1}\zeta_{cam}, \quad \tau = 0.04s .$$

If the high frequency measurement noise present in the signal ζ_{cam} is excessive, one can use a model based approximation of ζ_{cam}. We shall discussed this issue in the final section.

The compensator, which has been developed in continuous time, has been discretized for simulations. The sampling rate is chosen to be 10ms.

Fig. 4 shows the reduction of the torque fluctuation during cam transients achieved by the compensation. For this simulation run we have varied the reference cam independently from the throttle and engine speed (which are held constant). In this and all other simulations the MBT spark is used, that is $\sigma = 0$. Clearly, the compensator achieves a substantial level of disturbance attenuation. The disturbance rejection is not perfect because of the differences between the design and simulation models, discretization, and filtering used for the derivative of ζ_{cam}. The performance of the compensator appears much better if we look at its effect on drivability. Fig. 5 shows the performance of the compensated VCT engine compared with the conventional engine and uncompensated VCT engine. The input is the throttle step with the engine speed held constant and the cam reference scheduled on throttle and engine speed. The uncompensated VCT engine response is not monotonically increasing, indicating a drivability problem. Our compensation θ^*, which can be seen in the top plot in Fig. 5 as the difference between the solid and dashed curves, brings the response of the VCT engine close to that of the conventional engine, effectively removing this problem. We emphasize that the difference between the steady state values of the conventional engine and the (uncompensated) VCT engine has little effect on drivability. Rather, it is the shape

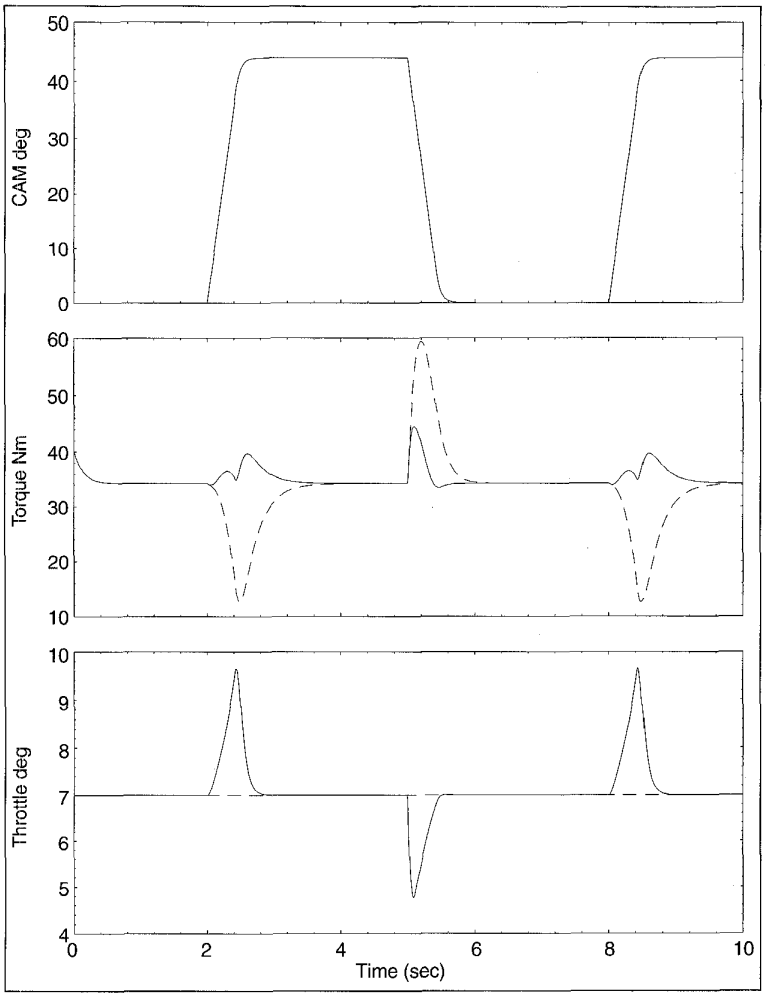

Fig. 4. Torque response of the VCT engine (dashed lines) to cam phase steps (0 to 44 deg.) at fixed engine speed (2000 RPM) and throttle angle (7 deg.); response with active compensation (full lines) shows substantial reduction in torque variation.

of the transient response which affects it the most. This observation will be used to modify our design objective in the next section, because low control authority of the air-bypass valve prevents us from recovering the torque response of the conventional engine.

Compensation with the Air-Bypass Valve

In the previous section we showed an effective way to modulate the electronic throttle to make a VCT engine respond like the conventional one. In most cases the engine will be equipped only with an air-bypass valve (ABV) which is used to control the idle speed by modifying the amount of air entering the intake manifold. We employ the ABV to affect the transients of the VCT engine and improve drivability.

Because an ABV has much smaller control authority than an ETC, we have to change our design objective: instead of trying to perfectly match the response of the conventional engine, we shall only try to modify the torque transient to have the same shape as that of a conventional engine. The steady state torque will be different, equal to that of the uncompensated VCT engine.

To explain this point, we refer to Fig. 6. The dashed and dotted curves show the static throttle-to-load (load is the normalized cylinder air charge) characteristics at a fixed engine speed for conventional ($\zeta_{cam} = 0°$) and fixed cam ($\zeta_{cam} = 35°$) engines. By scheduling the cam on the throttle and engine speed, we create a new static characteristic for the VCT engine shown by the solid curve in Fig. 6. Now our objective is to modify the transients of the VCT engine, using the ABV, so that the torque response is the same as that of a (fictitious) conventional engine which has a static throttle-to-load characteristic shown by the solid curve .

The new objective creates a problem for the design because now we do not have simple reference manifold pressure dynamics. In fact, as we change the throttle, the scheduled ζ_{ref} changes, and our reference manifold pressure model changes. We emphasize that it is not sufficient to introduce $F(N,P_m,\zeta_{ref})$ instead of $F(N,P_m,0)$ in the manifold pressure dynamics (8). The problem is that, at the step change in ζ_{ref}, not only must the dynamics for the reference pressure change, but also reference pressure value at that instant must change (jump). The generation of the desired reference manifold pressure can be done systematically at the expense of significant complexity. Instead, as a reference pressure we use the steady state value of the manifold pressure corresponding to the current values of N, θ_0, and ζ_{ref}. Simulation results have confirmed that the simplified algorithm performs very well.

With the air-bypass valve, the ideal gas law has to take into account the additional air coming through the ABV:

$$\dot{P}_m = K_m[g_1(P_m)(g_2(\theta_0)+g_3(\delta))-F(N,P_m,\zeta_{cam})], \tag{13}$$

where $\delta = \delta_0 + \delta^*$ is the opening of the air-bypass valve and g_3 is its static flow characteristic. We assign $\delta = 0$ to the completely closed and $\delta = 1$ to the completely open valve. Following the same steps as for the electronic throttle compensation, we obtain

$$\delta^* = g_3^{-1}\left(-\frac{\frac{\partial\alpha_1}{\partial\zeta_{cam}}P_m+\frac{\partial\alpha_2}{\partial\zeta_{cam}}}{K_m g_1(P_m)\alpha_1(N,\zeta_{cam}}\dot{\zeta}_{cam} + \frac{g_1(\bar{P}_m^{ss})}{g_1(P_m)}[g_2(\theta_0)+g_3(\delta_0)]\right)-\delta_0,$$

where, as we have said above, the reference pressure $\bar{P}_m^{ss} = \bar{P}_m^{ss}(N,\theta_0,\delta_0,\zeta_{ref})$ is the steady state value of the manifold pressure corresponding to the present values of the variables N, θ_0, δ_0, and ζ_{ref}. The evaluation of the reference pressure $\bar{P}_m^{ss}$ in real time can be done by evaluating two functions of two variables (two look-up tables).

The potential for instability for the compensation with the ABV is much smaller than with the ETC. The reasons are (i) at

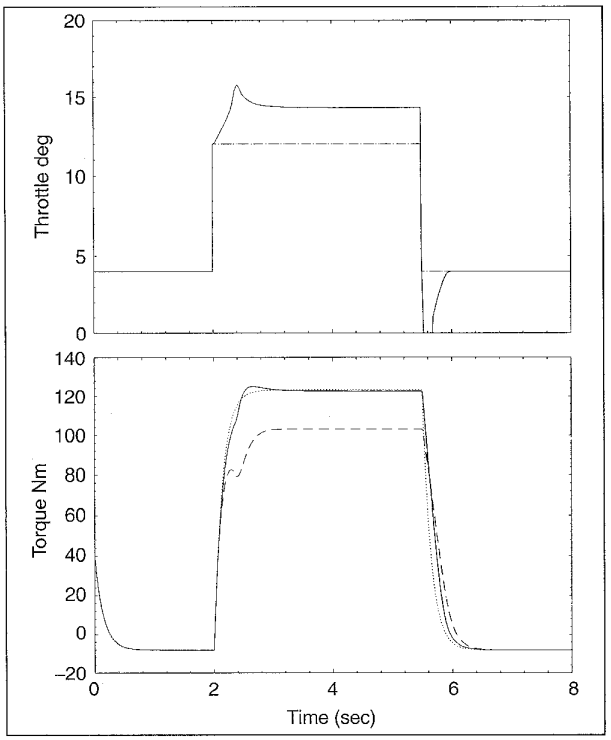

Fig. 5. Comparison of the throttle step torque response of the conventional engine (dotted lines), VCT engine without compensation (dashed lines), and VCT engine with compensation (full lines); engine speed is 2000 RPM, throttle is stepped from 4 to 12 and back to 4 deg.

the high end, $\overline{P}_m^{ss} < P_m^0$, and (ii) at the operating regimes with high manifold pressure, the ABV has little control authority. Nevertheless, we have used the skewed value $\hat{g}_1$ in the implementation.

The simulations are performed with the same simulation and design models as in the case of electronic throttle except that both models now include the air-bypass valve as an actuator. The air-flow characteristic of the valve is modeled as a sigmoidal function for the simulation model and as a straight line for the design model.

Plots in Fig. 7 show the air-bypass valve opening δ and the torque responses to throttle steps with the cam timing scheduled on throttle angle and engine speed. The torque of uncompensated VCT engine (dashed line) flares at both tip-ins and tip-outs indicating a drivability problem. Our compensation algorithm results in the torque response which closely resembles a scaled down response of the conventional engine (full line). The dynamics of the air-bypass valve have been neglected in the simulation model; the traces of δ for the uncompensated VCT engine show the dash-pot functionality of the air-bypass valve. The difference between the steady state values for two torques in Fig. 7 is due to the difference between the simulation and design models. It has no consequence on drivability and can be removed with a simple high-pass filter if desired.

The algorithm has shown very good performance in simulations The compensator has performed well over a variety of speed and load conditions. At high loads (high values of throttle) the air-bypass valve loses its control authority and the torque responses of the compensated and uncompensated engines are the same. However, this happens in the region where the VCT does not cause drivability problems.

Implementation of $\dot{\zeta}_{cam}$

Our compensation algorithms require that the derivative of ζ_{cam} be available. Two methods to obtain this derivative are explored. One method is to use the approximate differential of the available measurement as we have done for the simulations, the other one is a model based estimator. For the approximate differential, we use the a second order, low-pass Butterworth filter. The model based estimator uses ζ_{ref} and N as inputs to the model of the VCT mechanism (c.f. Fig. 2) which is itself a feedback loop consisting of the VCT actuator controlled by a PID regulator.

The VCT actuator system consists of a control valve and the actuator itself. This control oriented model captures the dominant behavior of the VCT actuator system. These dominant dynamics can be reduced to a single integrator. Adding higher frequency components does not add much to the accuracy of this model. The static control valve behavior is captured in the function $F(\cdot)$. It is purely a function of the control input. The gain of the VCT actuator depends heavily on the engine speed N and is described by the static function $K(N)$. A block diagram of the VCT mechanism model is shown in Fig. 8.

In Fig. 9, the estimated cam position and the cam position measured on the engine are the solid and dotted curve, respectively. The plot shows that the model captures the VCT mecha-

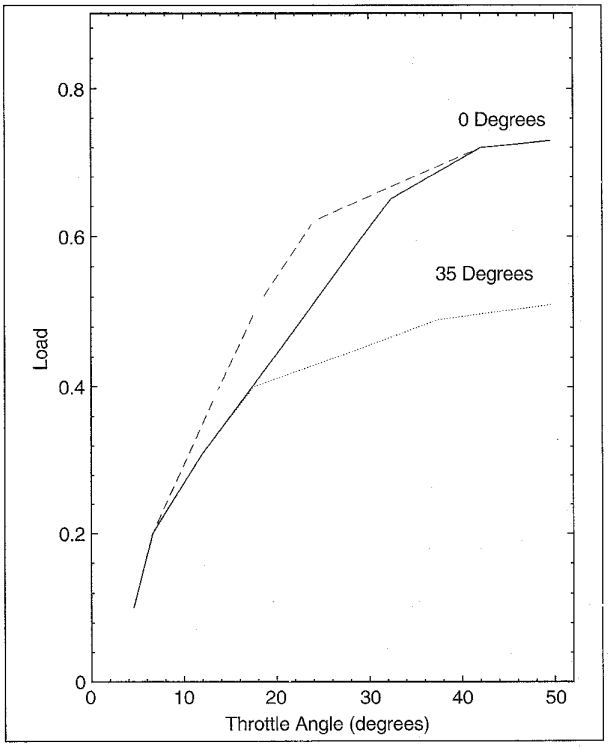

Fig. 6. Load vs throttle characteristic for the conventional engine (dashed line), an engine with cam fixed at 35° retard (dotted line), and the VCT engine with cam scheduled on throttle and engine speed (full line).

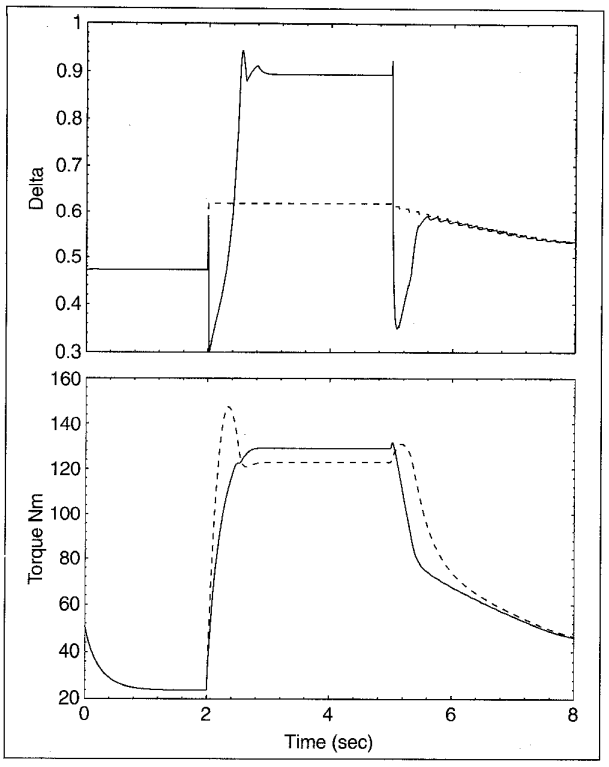

Fig. 7. Normalized air-bypass valve opening δ and torque response for the VCT engine without compensation (dashed lines) and with compensation (full lines); throttle steps 0 to 9 to 0 deg., engine speed 1250 RPM.

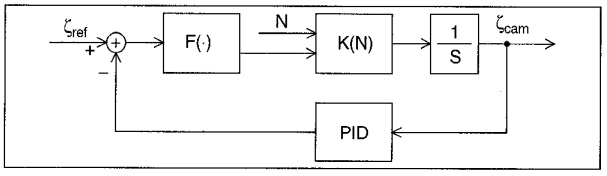

Fig. 8. Simplified controls-oriented model of the VCT mechanism.

nism dynamics very well. It also shows high frequency noise content in the measured signal which forces us to use a low bandwidth Butterworth filter for approximate differentiation.

The estimates of $\dot{\zeta}_{cam}$ obtained by two methods are shown in Fig. 10. The one obtained by differentiating the measured cam position lags the model-based one because of the low pass filtering and measurement delay. It appears that the model is sufficiently accurate to show a clear advantage over an approximate differentiation method. One must keep in mind, however, that this conclusion applies for the particular hardware implementation of the VCT sensor and actuator.

References

[1] T.W. Asmus, "Perspectives on Applications of Variable Valve Timing," SAE paper 910445, 1991.

[2] A. C. Elrod and M. T. Nelson, "Development of a Variable Valve Timing Engine to Eliminate the Pumping Losses Associated with Throttled Operation," SAE Paper No. 860537, 1986.

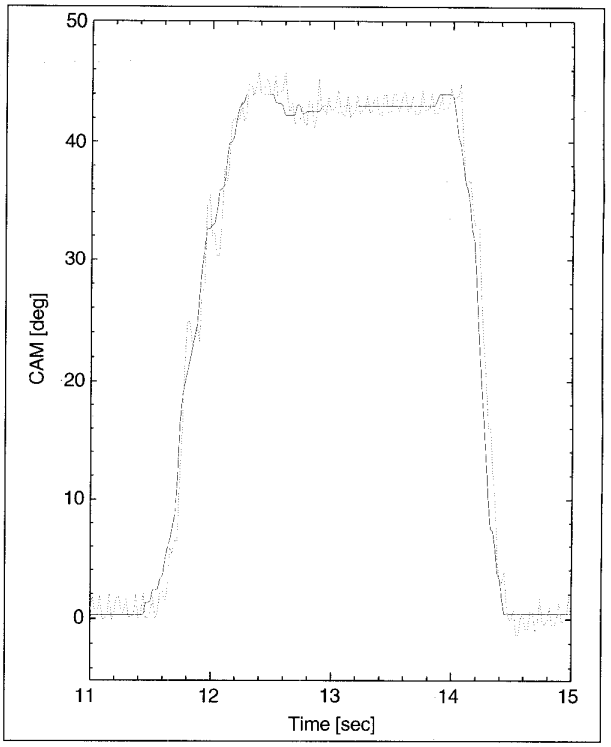

Fig. 9. Comparison of the model based ζ_{cam} estimate (solid) and ζ_{cam} measured (dotted).

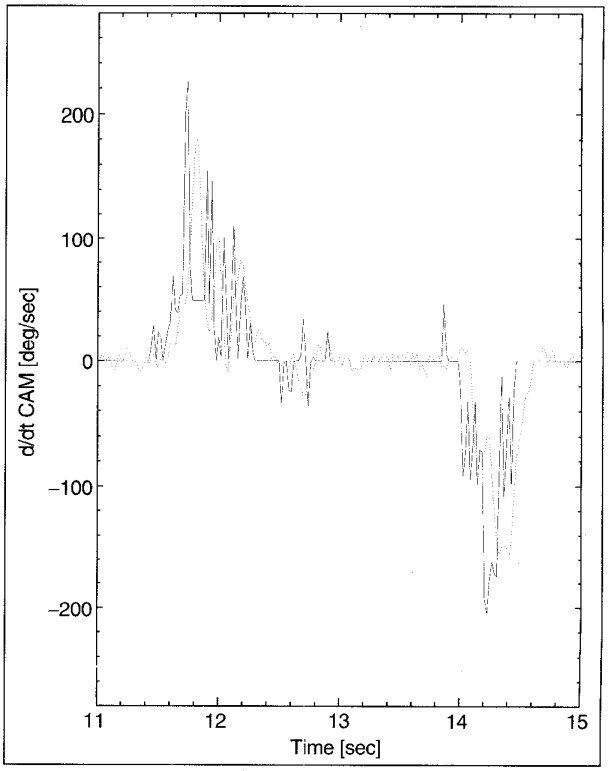

Fig. 10. Comparison of $\dot{\zeta}_{cam}$ estimate obtained by approximate differentiation (dotted) and the model based one (solid).

[3] A. L. Emtage, P. A. Lawson, M. A. Passmore, G. G. Lucas and P. L. Adcock, "The Development of an Automotive Drive-By-Wire Throttle System as a Research Tool", SAE Paper No. 910081, 1991.

[4] C. Gray, "A Review of Variable Engine Valve Timing," SAE Paper No. 880386, 1988.

[5] S. C. Hsieh, A. G. Stefanopoulou, J. S. Freudenberg, and K. R. Butts, "Emissions and Drivability tradeoffs in a Variable Cam Timing SI Engine with Electronic Throttle," *Proc. American Control Conf.*, 1997, pp.284–288.

[6] T.G. Leone, E.J. Christenson, R.A. Stein, "Comparison of Variable Camshaft Timing Strategies at Part Load," SAE paper 960584, 1996.

[7] T. H. Ma, "Effects of Variable Engine Valve Timing on Fuel Economy," SAE Paper No. 880390, 1988.

[8] G.-B. Meacham, "Variable Cam Timing as an Emission Control Tool," SAE Paper No. 700645, 1970.

[9] Y Moriya, A. Watanabe, H. Uda, H. Kawamura, M. Yoshiuka, "A Newly Developed Intelligent Variable Valve Timing System—Continuously Controlled Cam Phasing as Applied to New 3 Liter Inline 6 Engine," SAE paper 960579, 1996.

[10] B.K. Powell, J.A. Cook, "Nonlinear Low Frequency Phenomenological Engine Modeling and Analysis," *Proc. of American Control Conf., 1987*, pp.332–340.

[11] A. Stefanopoulou, K.R. Butts, J.A. Cook, J.S. Freudenberg, J.W. Grizzle, "Consequences of Modular Controller Development for Automotive Powertrains: A Case Study," *Proceedings of CDC*, New Orleans LA, 1995, pp. 768–773.

[12] A. Stefanopoulou, "Modeling and Control of Advance Technology Engines," Ph.D, Dissertation, University of Michigan, Ann Arbor MI, 1996.

[13] A.G. Stefanopoulou, J.A. Cook, J.W. Grizzle, J.S. Freudenberg, "Control-Oriented Model of a Dual Equal Variable Cam Timing Spark Ignition Engine, *ASME J. of Dynamical Systems, Measurement, and Control*, vol. 120, June 1998.

[14] R.A. Stein, K.M. Galietti, T.G. Leone, "Dual Equal VCT—A Variable Camshaft Timing Strategy for Improved Fuel Economy and Emissions," SAE Paper 950975, 1995.

[15] R. A. Stein, K. M. Galietti and T. G. Leone, "Dual Equal VCT- A Variable Camshaft Timing Strategy for Improved Fuel Economy and Emissions," SAE Paper No. 950975, 1995.

[16] J. H. Tuttle, "Controlling Engine Load by Means of Late Intake-Valve Closing," SAE Paper No. 800794, 1980.

Mrdjan Jankovic received the BS degree in Electrical Engineering from the University of Belgrade, Yugoslavia, and MS and D.Sc. degrees in Systems Science and Math from Washington University, St. Louis. He has held postdoctoral positions with Washington University and University of California, Santa Barbara. In 1995 he joined Ford Research Laboratories to work on development of advanced powertrain control systems. Dr. Jankovic's research interests include nonlinear and adaptive control with application to powertrain control systems. He has co-authored numerous technical articles and one book: *Constructive Nonlinear Control* (Springer-Verlag, 1997). Currently, Dr. Jankovic serves as an Associate Editor for *IEEE Transactions on Control Systems Technology.*

Florian Frischmuth was born in Berlin, Germany, in 1969. He received the B.S.E. and M.S.E. degrees in electrical engineering from The University of Michigan, Dearborn, MI in 1993 and 1995, respectively. He joined Ford Motor Company in 1993 as a Research Engineer concentrating in the areas of powertrain control and calibration in the Control Systems Department of the Ford Research Laboratory. In 1998 he joined the body E/E Subsystems Department, Advanced Vehicle Technology, as a Product Design Engineer. He is an IEEE Member.

Anna Stefanopoulou obtained her Diploma from the National Techical University of Athens, and her MS in Naval Archicture and Marine Engineering from the University of Michigan. She received a second MS and her Ph.D. in Electrical Engineering and Computer Science from the University of Michigan. She is presently an Assistant Professor at the Mechanical and Environmental Engineering Department at the University of California, Santa Barbara. Dr. Stefanopoulou is Vice-chair of the Transportation Panel in ASME DSCD and a recipient of a 1997 NSF CAREER award. Her research interests are in multivariable feedback control, controller architectures for industrial applications, and propulsion and powertrain modeling.

Jeffrey A. Cook joined the Ford Research Laboratories in 1976. He is a Staff Technical Specialist in the Powertrain Control Systems Department, where his research addresses systems and control development for advanced technology automotive powertrains.